

Pavol Durica - Peter Juras - Daniela Staffenova - Jan Rybarik*

LIGHTWEIGHT WOOD-BASED WALL: THE LONG-TIME EVALUATION OF HEAT-AIR-MOISTURE TRANSPORT

Five lightweight timber-frame wall sections with various thermal insulations and outdoor coating colors have been exposed to real outdoor boundary climate conditions since 2010. The indoor boundary conditions were set as constant. This article compares measured temperatures inside individual sections of the wall fragment to non-steady Heat-Air-Moisture (HAM) simulations in WUFI and ESP-r. The wall sections differ from each other in used thermal insulation: mineral wool, glass wool and hemp. Another difference is in color of outdoor surface: yellow, white and dark grey. Some wall compositions are equipped with vapor retarder. Each section has attached some thermal sensors.

Keywords: Platform frame, wood, experiment, HAM, moisture, thermal conductivity.

1. Introduction

Slovakia has a great potential for the construction of wooden buildings due to high forest coverage and wood availability. The number of wooden houses increases every year and has growth from 1% to 10% in around 5 years [1], but it is still low in comparison to Austria, Germany or Scandinavia (40 - 80 %). The natural conditions and increasing energy, ecology and economy requirements [2] created the need for long-term evaluation of different wooden structures, which are represented in this five sections of the experimental wall. The sandwich exterior wall fragment was designed and realized in all alternatives in the thermal-technical standard for passive buildings [2 and 3]. Comparing to standard structures, it differs from them in the inverse range of layers. The thermal-accumulating layer is situated from the exterior and the thermal-insulating layer is situated from the interior side of the wall fragment, so as we know it from some layer compositions used in Nordic countries [1].

2. Construction of the laboratory and experimental wall

Construction of the Laboratory Centre of the Department of Civil Engineering and Urban Planning started in 2010. Process of construction is shown in Figs. 1-5. The laboratory is constructed as a pavilion type and consists of two climatic chambers and office with recording equipment (Fig. 6). The chambers have controlled indoor environment (AC unit), which is set to maintain 20 °C

and 50% relative humidity at all the time. From the exterior, test wall sections were exposed to real boundary conditions of the external climate.

Later, since 2013, the laboratory center has been equipped also with detached experimental weather station, which records all necessary climatic parameters [4]. One climatic chamber has built-in lightweight wood-based experimental wall fragment, which consists of five different sections, the other one has three windows [5].



*Fig. 1 Beginning of construction work on the laboratory
- prepared opening for wooden frame (April 2010)*

Dimensions of monitored experimental wall fragment are 3670 x 2670 mm and it consists of 5 sections (Fig. 7). They differ

* Pavol Durica, Peter Juras, Daniela Staffenova, Jan Rybarik

Department of Building Engineering and Urban Planning, Faculty of Civil Engineering, University of Zilina, Slovakia
E-mail: pavol.durica@fstav.uniza.sk

from each other in material composition and surface coloring. Sections 1, 2, 4 and 5 are diffusional closed constructions and the third section is made as a diffusional open construction (Fig. 8). Detailed composition of the sections is shown in the Table 1. Used material properties are summarized in the Table 2. All compositions had to meet the requirements of Slovak standard STN 730540:2012, which is $U = 0.15 \text{ W/m}^2\text{K}$ after year 2020 (zero energy building). The main device for temperature measuring in tested sections is Ahlborn Almemo 5690-2M used as a datalogger with connected Ahlborn thermocouples (totally 22 pieces), which have deviation up to 0.4 K [6]. Some of the wall sections were later additionally equipped with combined temperature/relative humidity HUMI sensors and Raspberry Pi as a datalogger [7]. The thermocouples are generally located on the exterior surface, under the coating, on the internal surface of MDF board and on internal surface of the filling thermal insulation. Several sensors are located also on the wooden columns (Fig. 8). More detailed description is mentioned in [1 and 7]. The temperatures were recorded in 30 minutes time periods.



Fig. 2 View at wooden frame (May 2010)



Fig. 3 Montage of MDF board (September 2010)



Fig. 4 Montage of thermocouples on the wooden columns from inside (November 2010)

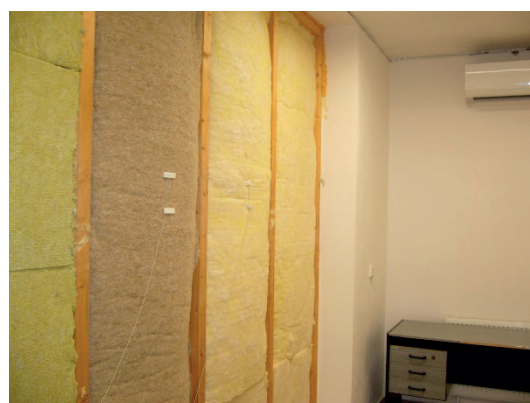


Fig. 5 Thermal insulation prior fitting vapor barrier (January 2011)



Fig. 6 View at data recording device ALMEMO 5690-2M in the office next to the laboratory rooms (May 2011)

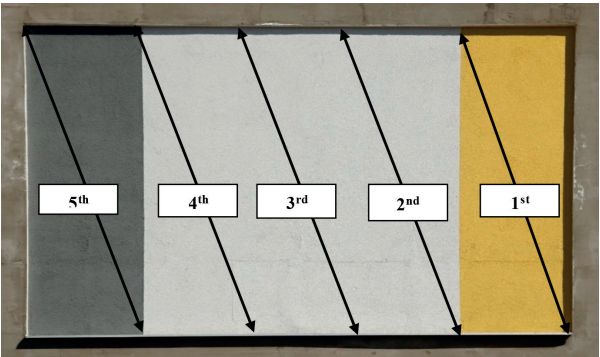


Fig. 7 Exterior view at the experimental wall fragment (3670 x 2760 mm) with marked five different sections (works were finished in November 2010)

The parameters of external environment were recorded by the detached experimental weather station at the same time step period (30 minutes) and captured were: temperature and relative humidity of external air, wind velocity and direction, the intensity of global solar radiation on a horizontal plane and the vertical plane identical to the orientation of the test wall fragment.

Evaluation of the wall structure

After the construction of the wall fragment and laboratory climatic chamber there were made several measurements made [1]. The outer surface temperatures were also measured with thermal camera several times. In the Fig. 10 is image from March

Composition of five sections within the experimental wall fragment

Table 1

Thickness [mm]	4	100	220	-	12
1 st section	Yellow coating	MDF board	Glass wool	Vapor barrier	OSB board
2 nd section	White coating		Hemp	-	
3 rd section				Vapor retarder with changeable permeability	
4 th section			Mineral wool		
5 th section	Grey coating				

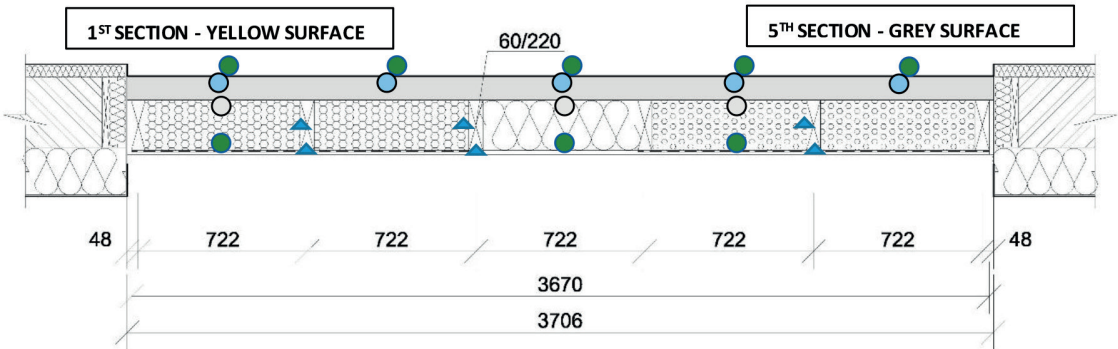


Fig. 8 Sketch showing measuring points in the construction of wall sections. Thermocouples: 1 - the exterior surface, 2 - under the coating, 3 - under the thermal insulation, 4 - under the infill thermal insulation, 5 - in the middle of the column, 6 - the inner surface of the column

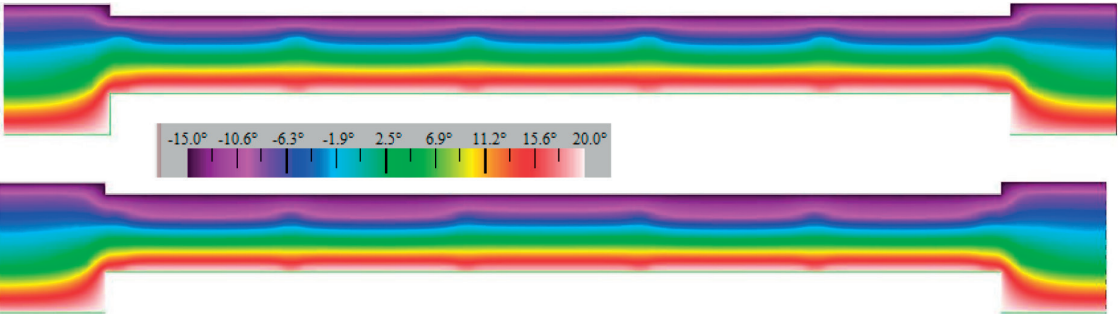


Fig. 9 Isotherm in the experimental wall fragment for boundary conditions $\theta_{a,i} = 20\text{ }^{\circ}\text{C}$, $\theta_{a,e} = -15\text{ }^{\circ}\text{C}$ in finite element simulator Therm v 5.2; Top: with usage of design thermal conductivities for materials (Table 2), bottom for measured conductivities in May 2015[8]; Noticeable is the decrease by MDF board across the wall and in 3rd section with Hemp

Material properties of used materials in the experimental wall

Table 2

MATERIAL	DESCRIPTION	d	λ	$\lambda_{current}$ [8]	ρ	c	μ
		m	W/(m.K)	W/(m.K)	kg/m ³	J/(kg.K)	-
External plaster	StoSilco	0.004	0.7	0.7	1900	720	40
Woodfiber MDF board	HofaTex SysTherm	0.1	0.045	0.10	210	2100	5
Stone wool insulation (MW)	Rockwool MW W	0.22	0.037	0.039	40	840	1
Hemp insulation	Cannabest Plus	0.22	0.040	0.039	36	1200	1.9
Glass wool insulation (GW)	Isover ENV	0.22	0.035	0.063	24	840	1
Vapour barrier with changeable diffusion resistance	Isover Vario KM Duplex	0.0004	1	-	2000	1470	90000
Vapour barrier	PE foil	0.0002	0.4	0.14	400	1470	10200
OSB board 3	OSB 3 MUPF/PMDI	0.012	0.14		700	2100	240

2011 after completing the thermal insulation layers. Exterior air temperature was -10 °C at around 4:00AM during measurement. In the figure are also shown the measured temperatures from thermocouples on the surface with the values obtained with the thermal camera, which showed very good match.

Long-term temperature measurement

To show long-term temperature measurement results in different layers of the wall fragment, a one week measurement during the winter season [9] from 27-01-2012 to 02-02-2012 was chosen ($\theta_{ae, min} = -18.9$ °C, $\theta_{ae, max} = 4.6$ °C). Outer surface temperatures of each section are shown in Fig. 11. Different temperatures in the structure were affected not only by its material composition, but also by natural influences of the environment as well as by the different light absorption and reflectance caused by various coating colors. The highest surface temperatures were measured on the dark coating. Such a coating has the lowest reflectivity of solar radiation and absorbs most short wave solar radiation. Maximum during clear days was above 48 °C, and higher by about 30 °C when we compared it to other surfaces. From sections with white coating, section no. 3 had the lowest surface temperature which is caused by the higher heat flow. During nights of the whole reference week, the surface temperature in all sections was lower than the ambient air temperature due to the cold sky radiation. At this time, the minimum temperatures were recorded mainly in the 4th section with white finish, and 1st section with yellow finish [9]. Significant influence of deviation of external conditions at the temperature course in the structure was noticed in monitored positions closest to the interior under the additional thermal insulation MDF board Hofatex. On the contact of the infill insulation with OSB board it was observed more significant impact of the technology of internal environment (AC unit used to maintain the indoor climate).

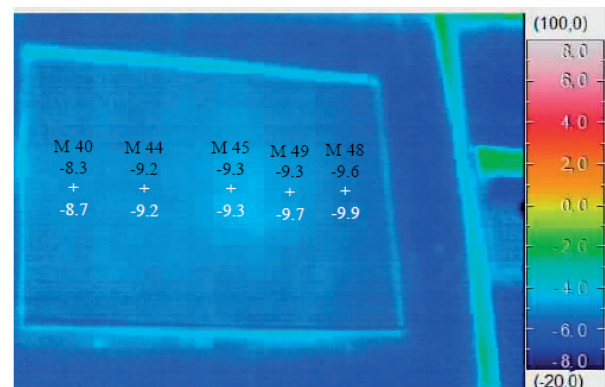


Fig. 10 Results from thermal camera NEC TH7700 measured on 09-03-2011, $\theta_{a,e} = -10$ °C; black values are from thermocouples on the surface, white are measured with thermal camera

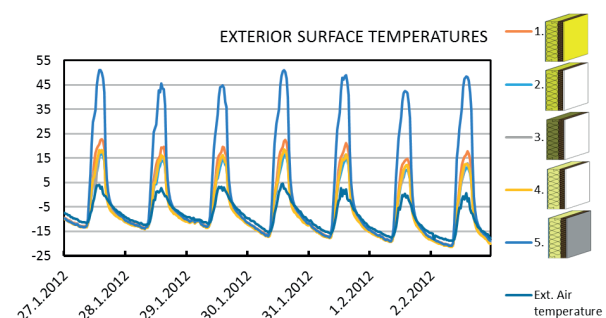


Fig. 11 Temperature courses at the exterior surface of the structure are from 27-01-2012 to 02-02-2012, surface finish coloring yellow (1st), white (2nd, 3rd and 4th) and dark grey (5th) [9]

During the winter period, the mechanism of heating and cooling process had positive effect on heat loss of the building, because minimum temperatures under the additional insulating layer and therefore the largest cooling of storage layer was thank to the thermal inertia and with it connected phase shift of the temperature oscillation recorded in time, when the experimental wall fragment was exposed to the solar radiation from the exterior side and therefore its energy was accumulated [1, 2 and 9].

Thermal conductivity measurements during exploitation

There were conducted measurements of thermal conductivity in the materials with use of Isomet 2104. By finding out properties of individual thermal insulations after 4 years from assembling it was observed that by 24-hour testing of thermal conductivity coefficient [10 and 11] of fibrous insulations this changed during the day only minimal or insignificantly (Table 3). By 24-hour testing in the additional insulation MDF board Hofatex, there were monitored significant changes in all sections, mostly in the 5th section with dark grey finish.

More significant changes were compared to the design or by manufacturer measured values. Based on measurements of water content in insulating materials, the following conclusions can be stated: The measured values of moisture in sections no. 1, 4 and 5 have no significant impact on the thermal conductivity of glass wool and mineral wool (infill insulations). The moisture of glass wool was measured 1.09 % and the thermal conductivity was measured max. 0.039 W/(m.K). The moisture of mineral wool was measured 3.47 % and the thermal conductivity 0.0402 W/(m.K), which are values close to the design values stated in [8]. These sections were constructed as diffusional closed constructions. On the other hand, moisture in section no. 3 has a big impact on the thermal conductivity of hemp insulation (11.63 %), because the design thermal conductivity of hemp insulation is 0.04 and the measured one is 0.0637 W/(m.K). That section was constructed as a diffusional open construction. The moisture has a big impact also on the thermal conductivity of MDF boards (moisture max. 13.42 %), the design value is 0.049 W/(m.K) (Table 2), but the maximal measured value is 0.129 W/(m.K) (Table 3).

Color of the façade surface has an impact on moisture content in MDF board but not on the individual layers of insulation

between wooden columns. The moisture in MDF boards under the dark grey plaster was on average 27 % lower than under the white plaster. Also moisture under the yellow plaster was lower but only an average of 9 % [9].

Measured values of moisture in 3rd and 4th section are nearly the same, which can be influenced by the moisture transport from the wetter 3rd section, because the MDF board is not separated between the individual sections.

The measured thermal conductivities have crucial impact on the thermal resistance of MDF board and hemp insulation in 3rd section. The difference in temperatures in the wall composition is shown in Fig. 9, calculated with measured and designed values in Therm software. Also comparisons in *U*-values and thermal resistance are summarized in Table 4. The *U*-value is lower in average about 20 % with exception in the 3rd section, where the *U*-value is lower by 42 %, which is a crucial finding.

Moisture measurements during exploitation

After three years of exploitation, in autumn 2014 (before the cold period of the year) and in spring 2015 (after the cold season of the year), the water content in thermal insulations, was measured. Mass moisture of MDF fibreboard and infill insulations was determined by the gravimetric method (STN EN ISO 12570/A1); mass moisture of wooden support poles by the resistance meter Greisinger GMH 3850. Gravimetric method is based on weighing wet and dry samples. Figure 13 shows the collection of samples for the gravimetric test, in this case from 5th section. Three samples were taken from each layer – the bottom, middle and top. From each section 9 samples were taken (1st, 2nd layer of infill insulation and MDF board). The difference between the positions in the layer was not significant. After being collected.

Measured thermal conductivities in the wall fragment materials. No measurement made in 2nd section

Table 3

	1 st section			3 rd section			4 th section			5 th section		
	thermal conductivity coefficient λ [W/(m.K)]											
Area of Insulation	min	max	Δ	min	max	Δ	min	max	Δ	min	max	Δ
infill insulation	0.039	0.039	0.001	0.062	0.064	0.002	0.038	0.040	0.003	0.038	0.039	0.001
MDF insulation	0.104	0.112	0.007	0.102	0.108	0.006	0.106	0.121	0.015	0.099	0.129	0.029

Comparison of designed and current thermal resistance *R* and *U*-value based on the thermal conductivity measurement (in the STN 73 0540:2012 is required 0.15 W/(m².K) after year 2020)

Table 4

	$R_{HOF,D}$	$R_{INS,D}$	$R_{HOF,C}$	$R_{INS,C}$	U_d	U_c	ΔU [%]
1 st section	2.22	5.95	1.00	5.64	0.122	0.151	18.70
2 nd section	2.22	6.29	1.00	5.64	0.118	0.151	21.94
3 rd section	2.22	5.50	1.00	3.49	0.129	0.223	41.83
4 th section	2.22	6.29	1.00	5.64	0.118	0.151	21.94
5 th section	2.22	6.29	1.00	5.64	0.118	0.151	21.94

the samples were put into a hermetic and vapor proof package and brought to the lab. The samples were weighed precisely before being placed into the drying oven. The drying oven Kendro-Heraeus was used for drying and the electronic scale Radwag PS 6000/C/2 was used for weighing (with an accuracy of 0.01 g). The drying temperature for insulating materials is 105 °C. After 24 hours of drying, samples were weighed, and drying and weighting cycles were repeated in 6 hour intervals. After reaching the constant weight of the samples, the cycle was completed and the values recorded. The difference in weight was equal to the amount of evaporated water.

Measurements of water content in sections 1, 4, 5 (in 2nd there were no measurements performed, because optical cables are used for the measurement and it is not possible to collect samples from it) in fibrous insulations confirmed constant low content [8] in both measured time periods. On the contrary, the increased water content was noticed in hemp layer with diffusional open compositions. The mass water content at the wool board oscillated in a range of 8.50% to 13.42%, while lower values were reached under darker surfaces (Fig. 14 - 1st and 5th). The highest moisture was recorded again in the part of the diffusional open construction (3rd).

By the wooden columns, the mass water content oscillated in a range of 10.00 to 15.20%, which are appreciative values for wood (columns are numbered as in Fig. 12, from the left to the right). Lower values were obtained at fronts of the columns from the interior side as at their sides – measured in the middle of columns (Fig. 13). With the same methodology the measurement was repeated in May 2015 after the cold period of the year. The comparisons of the measured values are shown in Fig. 13.

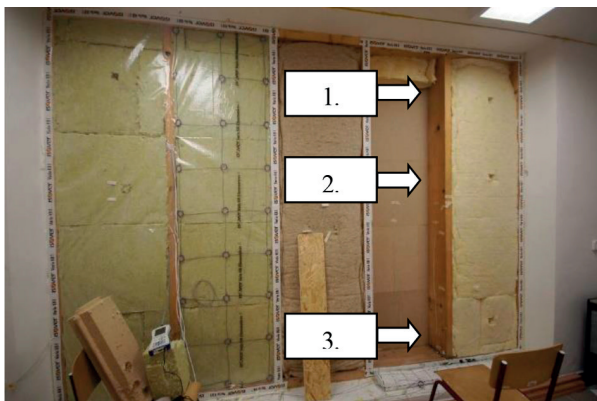


Fig. 12 Tested wall fragment from the interior during collecting of samples for the 5th section (in 2nd section optic cables are visible, we were not allowed to collect samples and do other measurements)

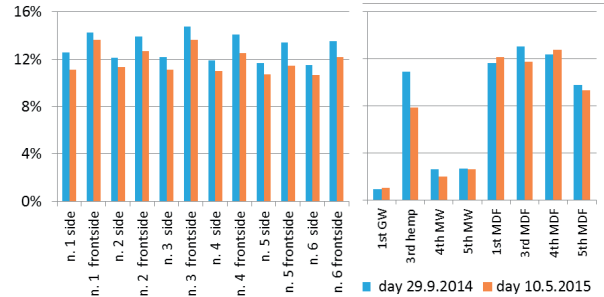


Fig. 13 Water content in wooden columns (left) and thermal insulations (right) in the wall composition

HAM simulation in WUFI and ESP-r

Two simulations were made. First were compared the measured temperatures through the wall fragments with calculation of temperatures with ESP-r, which is available via GPL-license. It has been the subject of sustained developments since 1974 with the objective of simulating the building performance and in this case uses finite volume method [12] and WUFI Pro [13], which also allows to calculate moisture transport and measured mass moisture from previous chapter was used. WUFI Pro allows calculation in multi-layer building components exposed to the natural weather of the transient coupled one dimensional heat and moisture transport described by Kunzel [14] (Eq. 1 and 2):

$$\frac{\partial H}{\partial \theta} \frac{\partial \theta}{\partial t} = \frac{\partial}{\partial x} \left(\lambda \frac{\partial \theta}{\partial x} \right) + h_v \frac{\partial}{\partial x} \left(\frac{\delta}{\mu} \frac{\partial p}{\partial x} \right) \quad (1)$$

$$\rho_w \frac{\partial u}{\partial \varphi} \frac{\partial \varphi}{\partial t} = \frac{\partial}{\partial x} \left(p_w D_w \frac{\partial w}{\partial \varphi} \frac{\partial \varphi}{\partial x} \right) + \frac{\partial}{\partial x} \left(\frac{\delta}{\mu} \frac{\partial p}{\partial x} \right) \quad (2)$$

- D_w is liquid transport coefficient [m²/s],
- H is enthalpy of the material [J/m³],
- h_v is enthalpy of the water [J/kg],
- p is partial pressure of water vapor [Pa],
- w is water volume in component [m³/m³],
- δ_A is water vapor diffusion coefficient in air [kg/(m.s.Pa)],
- θ is temperature [°C],
- λ is thermal conductivity coefficient [W/(m.K)],
- μ is water vapor diffusion resistance factor [-],
- ρ_w is bulk density of water [kg/m³],
- φ is relative air humidity [-].

It is based on the newest findings regarding vapor diffusion and liquid transport in building materials and it has been validated by detailed comparison with measurements obtained in the laboratory and on outdoor testing field [15].

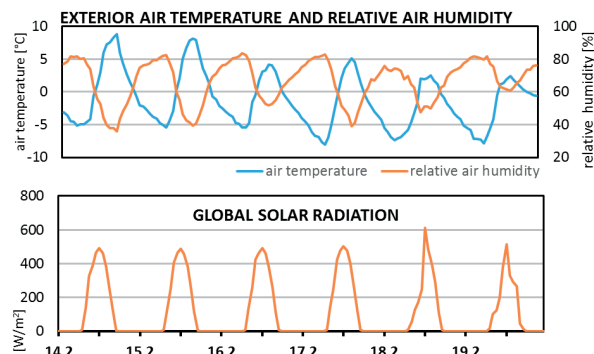


Fig. 14 Daily courses of air temperature, relative humidity (up) and global solar radiation (down) between the 14-02-2015 and the 19-02-2015 obtained by the detached experimental weather station [16]

As a basis for climate data, the measured data from the weather station were served. Different combinations of material properties from manufacturer's data sheets were used and compared to measured ones at the time of five years after completing the wall fragment. The thermal conductivity, especially, caused an increase of heat transfer and influenced the temperatures within the wall, which is significant for this comparison. The short-wave radiation absorptivity was used as 0.4 for yellow section and 0.6 for dark grey section. For calculating temperatures, the winter time period from the 14th of February to the 19th of February 2015, was used. The outdoor climate for the selected time period (Fig. 14) combines freezing temperatures (up to -10 °C) during the night with longwave radiation [17] and clear, sunny days which warmed the façade. The difference between the surface temperatures can be clearly seen.

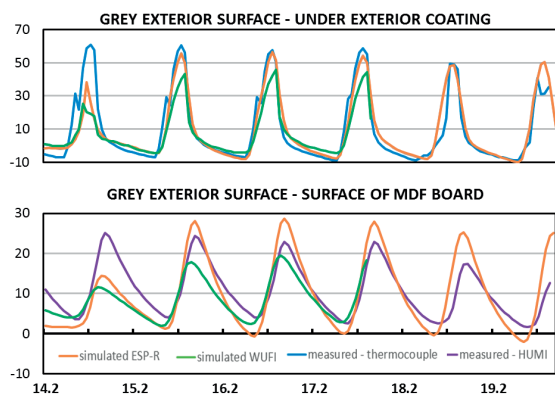


Fig. 15 Daily courses of temperature between the 14-02-2015 and the 19-02-2015 in the wall section with grey surface for positions under the exterior coating and inner surface of the MDF fiberboard [16]

Regarding the comparison of measurement and simulation, there is very good match between measurement and ESP-r for the temperatures under the exterior coating as shown in Fig. 15. This

shows that the handling of solar radiation by the numerical model is on high level. On the other hand, the WUFI calculates the day peaks temperatures around 10 K lower.

On the inner surface of MDF board, temperatures are slightly overestimated by ESP-r and underestimated by WUFI for dark grey surface.

It should be noted that after 4 years of assembly of the experimental wall fragment, the reflectance and short-wave solar radiation absorptivity is changed due to the dust and age. This comparison shows very good results for calculation of outdoor surface and undersurface temperatures, where the ESP-r obtained very good results. Disadvantage is the use of direct normal global solar radiation, which is not available in most cases and has to be approximated. In this comparison, WUFI mostly underestimates calculated temperatures, but this is on the safe side [16].

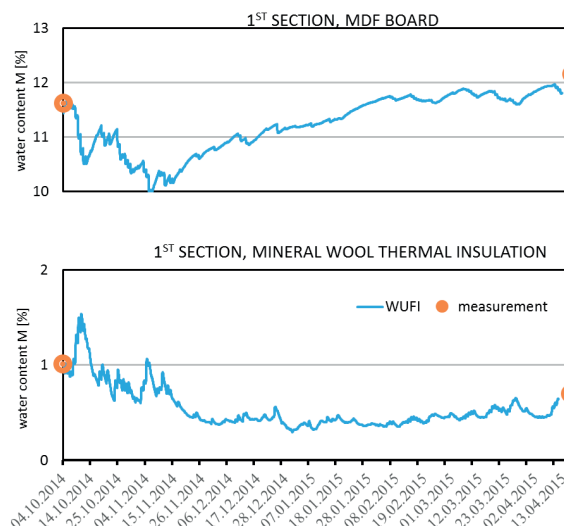


Fig. 16 Daily course of simulated water content (from 01-10-2014 to 10-05-2015) and results from the gravimetric measurement, 1st section [18]

The other simulation [18] incorporated WUFI software with measured outdoor climate from October 2014 to May 2015, measured initial water content in materials and thermal conductivities from previous chapters [8, 9]. The course of mass moisture is shown in Fig. 16.

Destruction, discussion and future

This long-term measurement of experimental wall fragment shows some rarely seen outputs. First of all, the high decrease of thermal resistance of the third section should be noticed. This is caused by the high moisture content in the hemp thermal insulation. On the other hand, in the rest of sections, there is not such a high impact of the exploitation to the outer climate. The

MDF board was not separated between sections, so the vapor diffusion and capillary water transport were possible inside the construction and it seems so, that it was there from the wetter third section. Another problem was the inner climate, because with current AC unit it was not possible to maintain the relative humidity in the room over the year constant. Another negative aspect was that there was no possibility to set direct value, if there was need to simulate another boundary condition such as kitchen or bathroom. Also the lack of funds causes no thermocouples inside the 5th section. The thermocouples provide good accuracy but there was also a lack of sensors for measuring relative humidity inside the fragments. This was later tried to improve with low-cost solution [7] with good results.

Nowadays is the wall dismantled and is being replaced by new one, which should reflect some consequences of these measurements, such as strictly divided sections, sensors for temperatures and relative humidity. The sections are more different, there will be also wood paneling with ventilated layer and massive wooden wall with inner thermal insulation. Also another climate room will be built with better AC unit with the possibility to set temperature and relative humidity strictly.

3. Conclusion

During long-term measurements it was shown as expedient to use the unconventional composition with inverse range of layers according to the model of Nordic countries in climate zone of central Europe too. The thermal-accumulative layer was warmed during winter days, which caused the improvement of boundary conditions for heat transport and decreasing heat loss. Moreover,

the negative influence of external environment was decreased (temperature extremes, UV radiation, dust, moisture, etc.) on filling fibrous thermal insulations, which thermal-insulating properties have not changed significantly during the day due to this fact. What is more, it was thus possible to avoid reinforcing OSB board from the exterior side, which has a positive impact not only on moisture transport through the structure, but in economic terms, the absence of one layer has positively influenced both - the amount of acquisition costs or labor content. The comparison of measurement results and simulations showed favorable accord in radiation model with ESP-r and moisture transport in WUFI.

Measured moistures in diffusional closed sections are low, without significant increase in thermal flow. In contrary is the section without vapor barrier (3rd), which thermal resistance decreases about 40% and its composition cannot be recommended for zero energy buildings and also does not complain the Slovak standard after five years of exploitation.

Based on the research course the conclusions for actions in lightweight wall in built-in state were formulated. However, it is needed to remark that these are valid for specific conditions of interior environment of air-conditioned room without presence of thermal gains from internal sources and without thermal gains from solar radiation through transparent constructions.

Acknowledgement

The research is supported by VEGA No. 1/0729/13 and VEGA 1/0945/16. Thanks to Caroline Kyzek, M.A. for language proofreading.

References

- [1] BADUROVA, S.: *Theoretical, Technical and Technological Aspects of the Design and Manufacturing of Wood-Based Buildings* (in Slovak). Dissertation thesis. Zilina, 2012.
- [2] PONECHAL, R., BADUROVA, S.: The Comparative Analysis of External Walls, a Passive House with Respect to Environment and Energy. *Advanced Materials Research: Buildings and Environment*, vol. 649, 2012, 129-132, ISSN 1022-6680.
- [3] DURICA, P. et al.: Energy and Environmental Evaluation of Selected Wooden Family Houses, *Communications - Scientific Letters of the University of Zilina*, No. 1, 2013, 88-95, ISSN 1335-4205.
- [4] STAFFENOVA, D. et al.: Climate Data Processing for Needs of Energy Analysis. *Advanced Materials Research: enviBUILD*, vol. 1041, 2014, 129-134, ISSN 1022-6680.
- [5] DURICA, P. et al.: Thermal Properties of Selected Lightweight Wooden Walls and Windows in the Regime of Long Time Testing, *Advanced Materials Research*, vol. 899 2014, 450-456, ISSN 1022-6680.
- [6] NiCr-Ni thermocouple T190-0, website < <http://ahlborn.com/getfile.php?2052.pdf> >
- [7] JURAS, P., SLAVIK, R.: Usage of Raspberry Pi for Temperature and Relative Humidity Measurements and Comparison with HAM Simulation, *Applied Mechanics and Materials*, vol. 824, 2016, 552-559, ISBN 978-3-03835-689-9.
- [8] DURICA, P. et al.: *Long-Term Monitoring of Thermo-Technical Properties of Lightweight Constructions of External Walls Being Exposed to the Real Conditions*, XXIV R-S-P seminar, Theoretical Foundation of Civil Engineering (24RSP), Procedia Engineering, 111, 2015, 176-182, ISSN 1877-7058.
- [9] SUSTIAKOVA, M., DURICA, P.: Monitoring Thermal Parameters of Lightweight Wood-Based Perimeter, *Advanced Materials Research*, vol. 1041, 2014, 315-318, ISSN 1022-6680.

- [10] ANDERSON, B. R.: *Conventions for U-Value Calculations*, 2nd ed., IHS - BRE Press. 2006, ISBN 1860819249.
- [11] ANDERSON, B. R.: *The Measurement of U-values on Site*, (online), homepage: <http://web.ornl.gov/sci/buildings/2012/1985%20B3%20papers/001.pdf>, (date of access: 2013-11-4).
- [12] ESP-r website < http://www.esru.strath.ac.uk/Programs/ESP-r_overview.htm>
- [13] WUFI website < <https://wufi.de/en/>>
- [14] KUNZEL, H. M.: *Simultaneous Heat and Moisture Transport in Building Components. One- and Two-dimensional Calculation using Simple Parameters*, Stuttgart : IBP Verlag, 1995.
- [15] DURICA, P., VERTAL, M.: Verification of the Water Transport Parameter - moisture Storage Function of Autoclaved Aerated Concrete - Approximately Calculated from a Small Set of Measured Characteristic Values, *Communications - Scientific Letters of the University of Zilina*, No. 4, 2011, 35-42, ISSN 1335-4205.
- [16] JURAS, P., PONECHAL, R.: Measurement of Lightweight Experimental Wall and Comparison with Different Simulation Programs, *Applied Mechanics and Materials*, vol. 820, 2016, 262-269. ISBN 978-3-03835-689-9.
- [17] CEKON, M.: Accuracy Analysis of Longwave Sky Radiation Models in the MZELWE Module of the ESP-r Program, *Energy and Building*, 103, 2015, 147 - 158, ISSN 0378-7788.
- [18] DURICA, P. et al.: *Lightweight Wood-Based Walls with Different Thermal Insulations: Long-Time Measurement and Subsequent Comparison with Ham Simulation*, Building Simulation, 14th Conference of IBPSA, 2015, 2371-2376, ISBN 978-93-5230-118-8.